Oxidative Addition Reactions of Saturated Si-X Bonds (X = H, F, C, or Si) to $Pt(PH_3)_2$. An ab Initio MO/MP4 Study

Shigeyoshi Sakaki* and Masami Ieki

Contribution from the Department of Applied Chemistry, Faculty of Engineering, Kumamoto University, Kurokami, Kumamoto 860, Japan. *Received July 27, 1992*

Abstract: Oxidative addition reactions of the saturated C-H, C-C, and Si-X bonds (X = H, F, C, or Si) to $Pt(PH_3)_2$ are theoretically investigated with the ab initio MO/MP4 method. The activation barrier (E_a) increases in the order Si-H (0.7) < Si-Si (17.4) < Si-F (25.8) < C-H (28.7) < Si-C (29.5) < C-C (60.7), while the exothermicity (E_{exo}) decreases in the order Si-Si (46.4) > Si-H (26.4) > Si-C (14.1) > C-C (0.9) > Si-F (-3.5) > C-H (-6.5), where the values in parentheses (MP4(SDQ) level: kcal/mol unit) represent either the E_a or the E_{exo} (the endothermicity is represented by a negative value). These results can explicate experimental findings that the Si-H and Si-Si oxidative additions proceed but the Si-F oxidative addition does not. The C-H, C-C, and Si-F reactions with $Pt(PH_3)_2$ are characterized as the typical oxidative addition, while the Si-H and Si-Si reactions with $Pt(PH_3)_2$ are considered as the rearrangement of covalent bonds rather than the oxidative addition. Electronic factors determining the exothermicity and the activation barrier are discussed in detail.

Introduction

Oxidative addition reactions of C-H and H-H σ-bonds to low-valent transition-metal complexes have received much attention in the last decade, because transition-metal alkyl and hydride complexes produced by these reactions play an important role as an active species and/or a key intermediate in many catalytic reactions.[1] In this regard, many theoretical investigations have been carried out on these reactions,[2-13] in an attempt to obtain information on the electronic factors controlling them. Oxidative addition reactions of Si-H, Si-Si, and similar saturated σ-bonds to the low-valent transition-metal complexes are also expected to be important in the syntheses of various Si compounds.[14-24] For instance, Pt(0)-disilene complexes, $Pt(PR_3)_2(SiR_2{=}SiR_2)$ and $[Pt(PR_3)_2]_2(SiR_2{=}SiR_2)$, have been synthesized via the Si-H oxidative addition to Pt(0).[18,19,24] The oxidative addition of the Si-Si σ-bond to Pd(0) is also considered as a key process in the palladium-catalyzed double sililation of olefin and acetylene.[17,22c,d] Additionally, the similar platinum(0) complex, $Pt(PEt_3)_3$, has been reported to undergo oxidative additions of the Si-I and Si-Si σ-bonds.[22b]

Although the oxidative addition of the Si-X σ-bond (X = H, C, halogen, or Si) to transition metals is important in the syntheses of Si compounds as described above, little effort has been made to clarify the electronic factors controlling the oxidative addition of the Si-X σ-bond, except for a few pioneering works.[25-27]

In our preliminary ab initio MO/MP4 work,[28] the oxidative addition of the Si-H bond to $Pt(PH_3)_2$ has been theoretically investigated, where striking differences between the Si-H and C-H oxidative additions have been pointed out. We now report a more detailed and systematic ab initio MO/MP4 study of the oxidative addition reactions (eq 1) of Si-H, Si-F, Si-C, Si-Si, C-H, and

$$X\text{-}EH_3 + Pt(PH_3)_2 \rightarrow cis\text{-}PtX(EH_3)(PH_3)_2 \quad (E = C \text{ or } Si) \tag{1}$$

C-C bonds to $Pt(PH_3)_2$. The following issues are mainly discussed: (1) the geometry and electronic structure of the transition state (TS), (2) changes in the electron distribution caused by these oxidative additions, (3) the comparison of the Si-X oxidative addition with the similar C-X oxidative addition, and (4) the

(1) For instance: (a) Crabtree, R. H. *The Organometallic Chemistry of the Transition Metals*; John Wiley: New York, 1988. (b) Shilov, A. E. *Activation of Saturated Hydrocarbons by Transition Metal Complexes*; D. Reidel: Dordrecht, 1984.

(2) For instance: (a) Dedieu, A. In *Topics in Physical Organometallic Chemistry*; Gielen, M. F., Ed.; Freund Publishing House: London, 1985; Vol. 1, p 1. (b) Koga, N.; Morokuma, K. In *Topics in Physical Organometallic Chemistry*; Gielen, M. F., Ed.; Freund Publishing House: London, 1989; Vol. 3, p 1. (c) Koga, N.; Morokuma, K. *Chem. Rev.* **1991**, *91*, 823.

(3) (a) Goddard, R. J.; Hoffmann, R.; Jemmis, E. D. *J. Am. Chem. Soc.* **1980**, *102*, 7667. (b) Tatsumi, K.; Hoffmann, R.; Yamamoto, A.; Stille, J. K. *Bull. Chem. Soc. Jpn.* **1981**, *54*, 1857. (c) Saillard, J.-Y.; Hoffmann, R. *J. Am. Chem. Soc.* **1984**, *106*, 2006.

(4) Jean, Y.; Eisenstein, O.; Volatron, F.; Maouche, B.; Sefra, F. *J. Am. Chem. Soc.* **1986**, *108*, 6587.

(5) (a) Kitaura, K.; Obara, S.; Morokuma, K. *J. Am. Chem. Soc.* **1981**, *103*, 2891. (b) Obara, S.; Kitaura, K.; Morokuma, K. *J. Am. Chem. Soc.* **1984**, *106*, 7482.

(6) Noell, J. O.; Hay, P. J. *J. Am. Chem. Soc.* **1982**, *104*, 4578.

(7) Low, J. J.; Goddard, W. J. *J. Am. Chem. Soc.* **1984**, *106*, 6928.

(8) (a) Blomberg, M. R. A.; Siegbahn, P. E. M. *J. Chem. Phys.* **1983**, *78*, 986. (b) Blomberg, M. R. A.; Siegbahn, P. E. M. *J. Chem. Phys.* **1983**, *78*, 5682. (c) Brandemark, U. B.; Blomberg, M. R. A.; Petterson, L. G. M.; Siegbahn, P. E. M. *J. Phys. Chem.* **1984**, *88*, 4617. (d) Blomberg, M. R. A.; Brandemark, U.; Siegbahn, P. E. M. *J. Am. Chem. Soc.* **1983**, *105*, 5557. (e) Blomberg, M. R. A.; Siegbahn, P. E. M.; Nagashima, U.; Wennergerg, J. *J. Am. Chem. Soc.* **1991**, *113*, 424.

(9) (a) Low, J. J.; Goddard, W. A. *J. Am. Chem. Soc.* **1984**, *106*, 8321. (b) Low, J. J.; Goddard, W. A. *Organometallics*, **1986**, *5*, 609. (c) Low, J. J.; Goddard, W. A. *J. Am. Chem. Soc.* **1986**, *108*, 6115.

(10) Hay, P. J. *J. Am. Chem. Soc.* **1987**, *109*, 705.

(11) Koga, N.; Morokuma, K. *J. Phys. Chem.* **1990**, *94*, 5454.

(12) Maseras, F.; Duran, M.; Lledos, A.; Bertran, J. *Inorg. Chem.* **1989**, *28*, 2984.

(13) Pacchioni, G. *J. Am. Chem. Soc.* **1990**, *112*, 80.

(14) (a) Patai, S., Rappoport, Z., Eds. *The Silicon-Heteroatom Bond*; Wiley: New York, 1991. (b) Corey, J. *Advances In Silicon Chemistry*; Larson, G., Ed.; JAI Press: Greenwich, CT, 1991; Vol. 1, p 325.

(15) (a) Colomer, E.; Corriu, R. J. P.; Marzin, C.; Vioux, A. *Inorg. Chem.* **1982**, *21*, 368. (b) Colomer, E.; Corriu, R. J. P.; Vioux, A. *Inorg. Chem.* **1979**, *18*, 695.

(16) (a) Luo, X.-L.; Crabtree, R. H. *J. Am. Chem. Soc.* **1989**, *111*, 2527. (b) Luo, X.-L.; Schulte, G. K.; Demou, P.; Crabtree, R. H. *Inorg. Chem.* **1990**, *29*, 4268.

(17) (a) Ito, Y.; Matsuura, T.; Murakami, M. *J. Am. Chem. Soc.* **1988**, *110*, 3692. (b) Murakami, M.; Anderson, P. G.; Suginome, M.; Ito, Y. *J. Am. Chem. Soc.* **1991**, *113*, 3987.

(18) (a) Zarate, E. A.; Tessier-Youngs, C. A.; Youngs, W. J. *J. Am. Chem. Soc.* **1988**, *110*, 4068. (b) Zarate, E. A.; Tessier-Youngs, C. A.; Youngs, W. J. *J. Chem. Soc., Chem. Commun.* **1989**, 577. (c) Anderson, A. B.; Shiller, P.; Zarate, E. A.; Tessier-Youngs, C. A.; Youngs, W. J. *Organometallics* **1989**, *8*, 2320. (d) Tessier, C. A.; Kennedy, V. O.; Zarate, E. A. *Inorganic and Organometallic Oligomers and Polymers*; Harrod, J. F., Laine, R. M., Eds.; Klumer Press: Amsterdam, 1991; p 13.

(19) (a) Pham, E. K.; West, R. *J. Am. Chem. Soc.* **1989**, *111*, 7667. (b) Pham, E. K.; West, R. *Organometallics*, **1990**, *9*, 1517.

(20) Schubert, U.; Muller, C. J. *J. Organomet. Chem.* **1989**, *373*, 165.

(21) Thorn, D. L.; Harlow, R. L. *Inorg. Chem.* **1990**, *29*, 2017.

(22) (a) Hayashi, T.; Kawamoto, A. M.; Kobayashi, T.; Tanaka, M. *J. Chem. Soc., Chem. Commun.* **1990**, 563. (b) Yamashita, H.; Kobayashi, T.; Hayashi, T.; Tanaka, M. *Chem. Lett.* **1990**, 1447. (c) Hayashi, T.; Kobayashi, T.; Kawamoto, A. M.; Yamashita, H.; Tanaka, M. *Organometallics* **1990**, *9*, 280. (d) Yamashita, H.; Catellani, M.; Tanaka, M. *Chem. Lett.* **1991**, 241. (e) Yamashita, H.; Kobayashi, T.; Hayashi, T.; Tanaka, M. *Chem. Lett.* **1991**, 761. (f) Sakakura, T.; Lautenschlager, H.-J.; Nakajima, M.; Tanaka, M. *Chem. Lett.* **1991**, 913.

(23) Harrod, J. F.; Mu, Y.; Samuel, E. *Polyhedron* **1991**, *10*, 1239.

(24) Heyn, R. H.; Tilley, T. D. *J. Am. Chem. Soc.* **1992**, *114*, 1917.

(25) Lichtenberger, D. L.; Rai-Chaudhuri, A. *J. Am. Chem. Soc.* **1989**, *111*, 3583.

(26) Rabaa, H.; Saillard, J.-Y.; Schubert, U. *J. Organomet. Chem.* **1987**, *330*, 397.

(27) Harrod, J. F.; Ziegler, T.; Tschinke, V. *Organometallics* **1990**, *9*, 897.

(28) Sakaki, S.; Ieki, M. *J. Am. Chem. Soc.* **1991**, *113*, 5063.

0002-7863/93/1515-2373$04.00/0

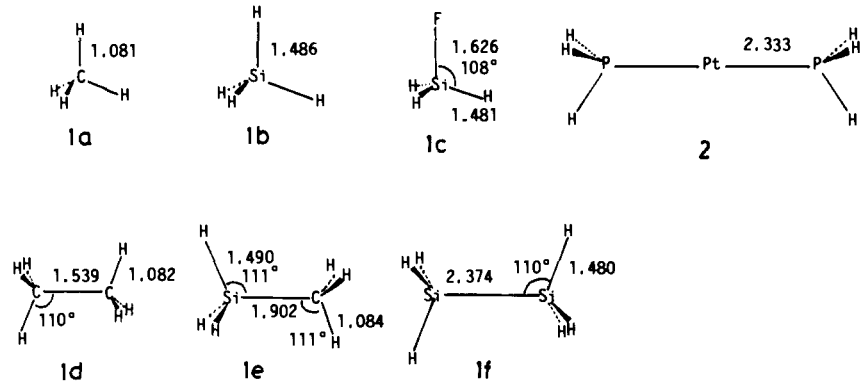

Figure 1. Optimized geometries of reactants: bond lengths in Å and angles in deg.

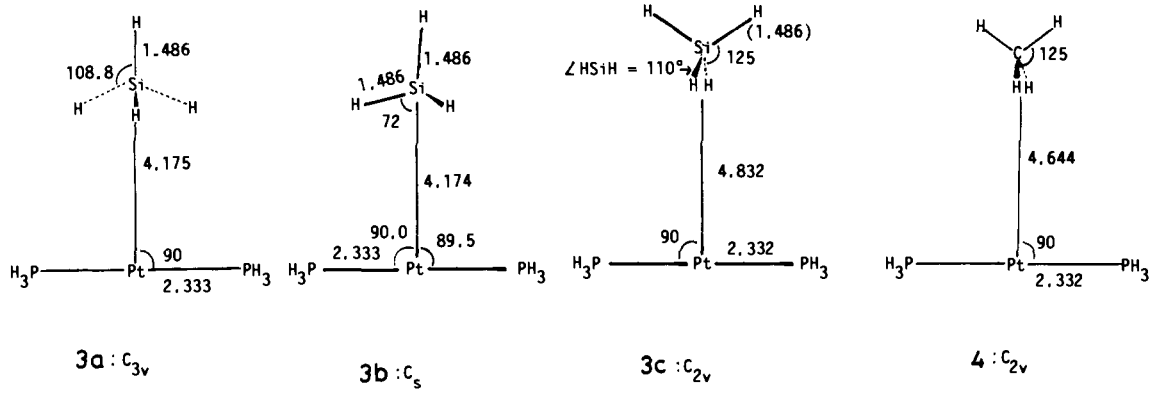

Figure 2. Optimized geometries of precursor complexes, $Pt(PH_3)_2(SiH_4)$ and $Pt(PH_3)_2(CH_4)$: bond lengths in Å and bond angles in deg. In parentheses is the assumed value which is taken to be the same as in the free molecule.

electronic factors controlling the exothermicity and the activation energy.

Computational Details

Ab initio closed-shell Hartree–Fock (HF) and MP4 calculations were carried out with Gaussian 82[29] and 86[30] programs. Two kinds of basis sets, BS-I and BS-II, were employed. The BS-I set was used only for optimizing geometries at the HF level, and the BS-II set was used for MP2–MP4 calculations. In the BS-I set, the 5s, 5p, 5d, 6s, and 6p orbitals of Pt were represented by a (5s 5p 3d)/[3s 3p 2d] set, where inner core orbitals of Pt were replaced by the relativistic effective core potential (ECP) of Hay and Wadt.[31] For ligand atoms, MIDI-3 basis sets were used,[32a] except for MINI-I sets employed for PH_3.[32a,b] In the BS-II set, the 5s, 5p, 5d, 6s, and 6p orbitals of Pt were represented by a (5s 5p 3d)/[3s 3p 3d] set, where the inner core orbitals of Pt were replaced by the same ECP as in the BS-I set.[31] For all the ligand atoms, MIDI-4 basis sets were employed.[32a] In both BS-I and BS-II, the basis set of Si was augmented with a d-polarization function.[32c]

Geometries were optimized with the energy gradient technique at the HF level, where the geometry of PH_3 was taken from the experimental structure of the free PH_3 molecule.[33] Structures of the TS were located by calculating the Hessian matrix. MP2–MP4 calculations were performed with all the core orbitals excluded. The basis set superposition error (BSSE) was corrected at the HF level by the method of Boys and Bernardi.[34]

Results and Discussion

C–H and Si–H Oxidative Addition Reactions. Optimized geometries of reactants and precursor complexes (PCM) are shown in Figures 1 and 2, respectively. In the PCM of $Pt(PH_3)_2(SiH_4)$, C_{2v} (**3a**), C_{3v} (**3b**), and C_s (**3c**) structures[35] are examined (see Figure 2 for **3a–c**). **3a** and **3b** are calculated to exhibit almost the same stabilization energy and to be slightly more stable than **3c** by 1.4 kcal/mol at the MP4 (SDQ) level. In $Pt(PH_3)_2(CH_4)$, the C_{2v} (**4**) structure is calculated to be only 0.1 kcal/mol more stable than the C_{3v} structure (HF/BS-II calculations), where the C_s structure was not examined because both C_s and C_{3v} structures yielded almost the same stabilization energy in $Pt(PH_3)_2(SiH_4)$ (vide supra). In these PCM's, geometries of $Pt(PH_3)_2$, SiH_4, and CH_4 parts deviate little from their isolated structures (Figure 1). At the same time, the interfragment distance between $Pt(PH_3)_2$ and SiH_4 (or CH_4) is too long to form a usual coordinate bond. Corresponding to these features, stabilization energies of these PCM's are very small, as shown in Table I (only the most stable structure is given there). Thus, these PCM's are considered as a van der Waals complex. Because of the very shallow stabilization energies, it is ambiguous that these PCM's exist on the potential surface of the reaction.

Geometries of the TS and products are shown in Figures 3 and 4, respectively. At the TS, both CH_4 and SiH_4 approach Pt with the H atom in the lead. With the exception of this common feature, geometries of the TS present several striking contrasts

(29) (a) Binkley, J. S.; Frisch, M.; Raghavachari, K.; DeFrees, D.; Schlegel, H. B.; Whiteside, R.; Fluder, E.; Seeger, R.; Pople, J. A. Gaussian 82; Carnegie-Mellon University: Pittsburgh, PA, 1983. Several subroutines for effective core potential calculation supplied by P. J. Hay and new computational method of electron repulsion integrals supplied by S. Obara[29b] were added to Gaussian 82 by N. Koga and K. Morokuma. (b) Obara, S.; Saika, A. *J. Chem. Phys.* **1986**, *84*, 3963. Obara, S.; Honda, M.; Nakano, H.; Sakano, F.; Takada, S.; Miyake, Y. KOTO, a library program of the computer center of the Institute for Molecular Science.

(30) Frisch, M. J.; Binkley, J. S.; Schlegel, H. B.; Raghavachari, K.; Melius, C. F.; Martin, R. L.; Stewart, J. J. P.; Bobrowicz, F. W.; Rohlfing, C. M.; Kahn, L. R.; DeFrees, D. J.; Seeger, R.; Whiteside, R. A.; Fox, D. J.; Fluder, E. M.; Topiol, S.; Pople, J. A. Gaussian 86; Carnegie-Mellon Quantum Chemistry Publishing Unit, Carnegie-Mellon University: Pittsburgh PA, 1987.

(31) Hay, P. J.; Wadt, W. R. *J. Chem. Phys.* **1985**, *82*, 299.

(32) (a) Huzinaga, S.; Anzelm, J.; Klobukowski, M.; Radio-Andzelm, E.; Sakai, Y.; Tatewaki, H. *Gaussian Basis Sets for Molecular Calculations*; Elsevier: Amsterdam, 1984. (b) Dunning, T. H. *J. Chem. Phys.* **1970**, *53*, 2823. (c) Sakai, Y.; Tatewaki, H.; Huzinaga, S. *J. Comput. Chem.* **1981**, *2*, 108.

(33) Herzberg, G. *Molecular Spectra and Molecular Structure*; Academic Press: New York, 1974; Vol. 3, p 267.

(34) Boys, S. F.; Bernardi, F. *Mol. Phys.* **1970**, *19*, 553. Ostlund, N. S.; Merrifield, D. L. *Chem. Phys. Lett.* **1976**, *39*, 612.

(35) Strictly speaking, the total symmetry is C_s. However, these names are adopted here regarding only the Pt–SiH_4 (or Pt–CH_4) part.

Table I. Energy Changes in Oxidative Addition (kcal/mol unit)[a]

	HF	MP2	MP3	MP4(DQ)	MP4(SDQ)
		(A) C–H Oxidative Addition			
sum of reactants[b]	−842.4714	−842.8505	−842.8735	−842.8972	−842.9065
precursor complex[c]	−0.1 (0.1)[d]	−0.6 (−0.4)[d]	−0.6 (−0.4)[d]	−0.6 (−0.4)[d]	−0.6 (−0.4)[d]
TS	47.3 (49.6)	25.9 (28.2)	30.7 (33.0)	29.2 (31.5)	28.1 (30.4)
product	19.1	5.2	9.3	6.3	6.5
		(B) Si–H Oxidative Addition			
sum of reactants[d]	−1093.2306	−1093.5960	−1093.6242	−1093.6483	−1093.6583
precursor complex[c]	−0.6 (0.2)	−2.2 (−1.4)	−2.2 (−1.4)	−2.2 (−1.3)	−2.3 (−1.5)
TS	11.1 (13.4)	−1.9 (0.4)	1.9 (4.2)	0.1 (2.4)	−1.6 (0.7)
product	−9.6	−27.3	−25.3	−25.6	−25.6
		(C) Si–F Oxidative Addition			
sum of reactants[b]	−1192.7002	−1192.5165	−1192.5329	−1192.5599	−1192.5722
precursor complex[c]	−3.0 (−1.3)	−5.8 (−4.0)	−5.6 (−3.9)	−5.6 (−3.9)	−6.0 (−4.2)
TS	39.7 (46.7)	19.7 (26.7)	22.1 (29.1)	21.9 (28.9)	19.8 (26.8)
product	−11.9	−29.8	−27.8	−28.3	−28.5
		(D) C–C Oxidative Addition			
sum of reactants[b]	−881.4443	−881.9128	−881.9448	−881.9706	−881.9800
precursor complex[c]	−0.2 (0.1)	−1.1 (−0.8)	−1.1 (−0.8)	−1.1 (−0.8)	−1.1 (−0.8)
TS	92.0 (94.4)	65.5 (68.0)	72.3 (74.8)	69.8 (72.3)	66.0 (68.5)
product	21.8	2.4	4.5	5.8	5.2
		(E) Si–C Oxidative Addition			
sum of reactants[b]	−1132.2219	−1132.6775	−1132.7135	−1132.7394	−1132.7497
precursor complex[c]	−0.5 (0.3)	−2.2 (−1.3)	−2.1 (−1.2)	−2.0 (−1.1)	−2.3 (−1.4)
TS	45.2 (48.4)	24.1 (27.3)	29.3 (32.5)	27.5 (30.7)	24.9 (28.1)
product	6.8	−16.5	−13.1	−13.4	−14.1
		(F) Si–Si Oxidative Addition			
sum of reactants[b]	−1382.9856	−1383.4318	−1383.4752	−1383.5015	−1383.5124
precursor complex[c]	−1.6 (−0.5)	−3.7 (−2.6)	−3.6 (−2.4)	−3.5 (−2.4)	−3.7 (−2.6)
TS	31.1 (34.4)	13.6 (16.9)	18.1 (21.4)	16.4 (19.7)	13.7 (17.0)
product	−19.7	−50.5	−42.3	−45.0	−46.4

[a] A negative value means stabilization in energy. [b] Sum of total energies of reactants (hartree unit). [c] Stabilization energy for the most stable structure is given. [d] In parentheses, the basis set superposition error is corrected.

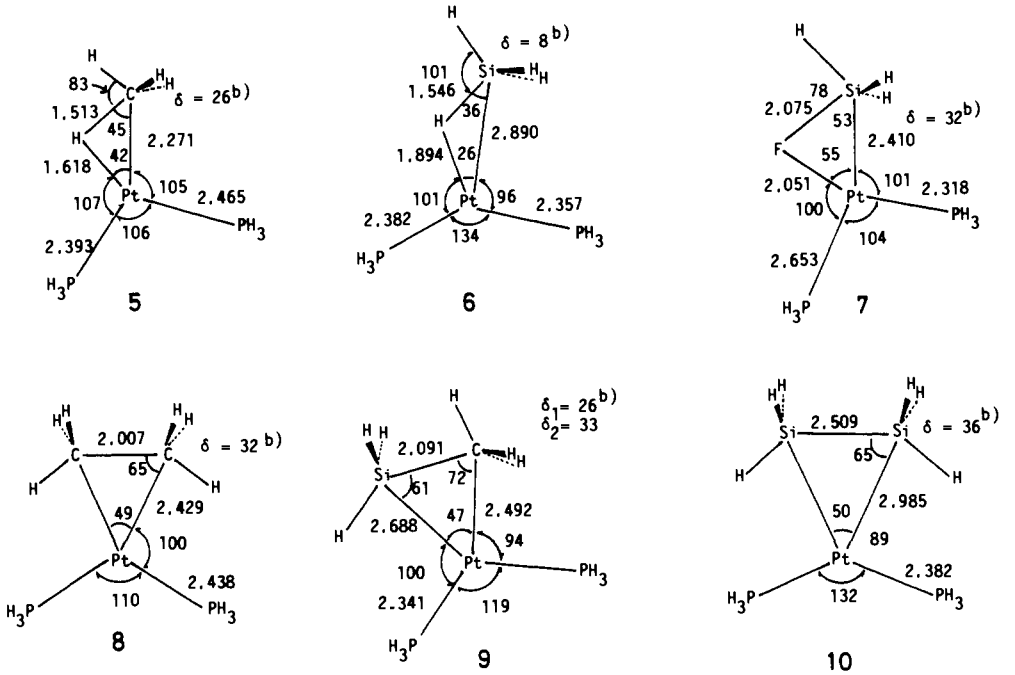

Figure 3. Optimized structures of transition state in C–H, Si–H, Si–F, C–C, Si–C, and Si–Si oxidative additions: bond lengths in Å and bond angles in deg. A "b)" designates a change in the EH_3 orientation (E = C or Si) from the E–H bond.

between the C–H and Si–H oxidative additions: (1) in the TS of the C–H oxidative addition, the Pt–C and Pt–H distances and the PPtP angle are similar in magnitude to those in the product, and the C–H bond substantially lengthens (see **5** in Figure 3); (2) in the TS of the Si–H oxidative addition, on the other hand, the Pt–Si and Pt–H distances are still long, the PPtP angle does not yet close so much, and the Si–H bond lengthens only a little (see **6** in Figure 3). These features indicate that the C–H oxidative addition gets to the TS relatively late, but the Si–H oxidative addition reaches the TS relatively early.

Activation energies and exothermicities of these oxidative additions are given in Table I. Inclusion of the electron correlation significantly decreases the activation barrier, as expected, and increases the exothermicity (or decreases the endothermicity). The discussion presented is, therefore, based on the results at the correlated level. Again, the Si–H oxidative addition provides a

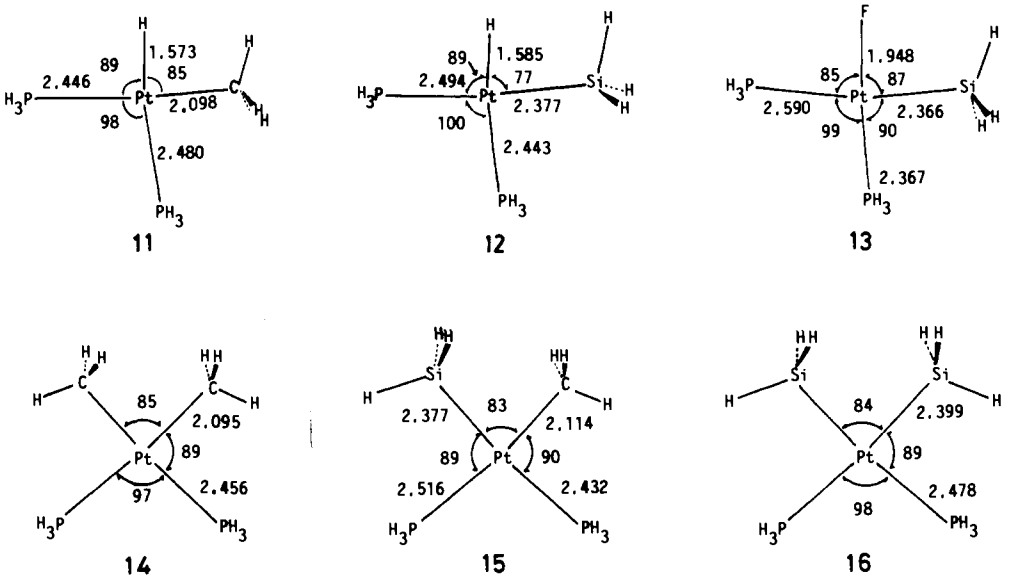

Figure 4. Optimized geometries of products: bond distances in Å and bond angles in deg.

Table II. Estimated Bond Energies (kcal/mol)

	E(H–CH_3)	E(H–SiH_3)	E(F–SiH_3)	E(CH_3–CH_3)	E(SiH_3–CH_3)	E(SiH_3–SiH_3)	E(Pt–H)[h]	E(Pt–F)	E(Pt–CH_3)	E(Pt–SiH_3)
MP2	99.0	82.9	129.3	86.8	82.7	72.9	52.3	61.3	42.2	64.4
MP3	99.0	84.2	120.8	84.9	80.9	73.2	54.7	57.3	40.2	60.3
MP4/DQ	99.9	84.5	122.1	84.6	80.2	72.5	54.7	58.4	39.4	59.4
MP4/SDQ	100.0	84.6	123.4	84.6	80.5	72.7	54.2	59.2	39.7	61.5
exptl	104.8[a]	90.3[b]	154[e]	88[f]	88.2[f]	74[f]				
other theor.										
MP4SDTQ/6-31G**		91.3[c]	144.3[d]							
		91.8[d]								
+ZPE[g]		85.7[d]	138.8[d]							

[a] Reference 38. [b] Reference 39. [c] Reference 40. [d] Reference 41. [e] Reference 42. [f] Reference 43. [g] Zero-point energy is corrected. [h] Reference 37b.

striking contrast to the C–H oxidative addition, as follows: the former is significantly exothermic and its activation barrier is very small,[36] while the latter is moderately endothermic and its activation barrier is considerably high. This contrast is consistent with the above-described difference in the TS; i.e., the C–H oxidative addition reaches the TS relatively late, but the Si–H oxidative addition gets to the TS relatively early.

The differences of these oxidative additions could be related to the strength of the Si–H, C–H, Pt–H, Pt–SiH_3, and Pt–CH_3 bonds. Their bond energies are estimated by considering the assumed reactions described below (an estimation of the Pt–F and Si–F bond energies is also given here, for brevity).

$$CH_4 \rightarrow {}^{\bullet}CH_3 + {}^{\bullet}H \quad (2)$$

$$CH_3\text{–}CH_3 \rightarrow 2{}^{\bullet}CH_3 \quad (3)$$

$$SiH_4 \rightarrow {}^{\bullet}SiH_3 + {}^{\bullet}H \quad (4)$$

$$SiH_3F \rightarrow {}^{\bullet}SiH_3 + {}^{\bullet}F \quad (5)$$

$$SiH_3\text{–}CH_3 \rightarrow {}^{\bullet}SiH_3 + {}^{\bullet}CH_3 \quad (6)$$

$$SiH_3\text{–}SiH_3 \rightarrow 2{}^{\bullet}SiH_3 \quad (7)$$

$$Pt(PH_3)_2 + 2{}^{\bullet}H \rightarrow cis\text{-}Pt(H)_2(PH_3)_2 \quad (8)$$

$$Pt(PH_3)_2 + CH_3\text{–}CH_3 \rightarrow cis\text{-}Pt(CH_3)_2(PH_3)_2 \quad (9)$$

$$Pt(PH_3)_2 + SiH_3\text{–}SiH_3 \rightarrow cis\text{-}Pt(SiH_3)_2(PH_3)_2 \quad (10)$$

$$Pt(PH_3)_2 + F\text{–}SiH_3 \rightarrow cis\text{-}Pt(F)(SiH_3)(PH_3)_2 \quad (11)$$

In the estimation, radicals were calculated with the UHF/UMP4 method by using the BS-II set, where their geometries were optimized by UHF/BS-I calculations. Although the Pt–F bond energy can be estimated by considering eq 12, thus-estimated value

$$Pt(PH_3)_2 + F_2 \rightarrow cis\text{-}Pt(F)_2(PH_3)_2 \quad (12)$$

would involve a substantial error, probably because F_2 cannot be computed well by MP4(SDQ)/BS-II calculations.[37a] Therefore, eq 11 was used for estimating the Pt–F bond energy. As listed in Table II, bond energies of H–CH_3, H–SiH_3, CH_3–CH_3, SiH_3–CH_3, and SiH_3–SiH_3 are more or less underestimated by ca. 2–8 kcal/mol. These errors do not seem, however, too large by considering the quality of the BS-II set. Unfortunately, the F–SiH_3 bond energy is underestimated more than the others, which further leads to underestimation of the Pt–F bond energy because

(36) In the Si–H oxidative addition, the moderately large activation energy at the HF level almost disappears at the correlated level. This means that the TS is more reactant-like at the correlated level than at the HF level.

(37) (a) E(F–F) is estimated to be only 13.0 kcal/mol at the MP4(SDQ) level, which is much lower than the experimental value (36.95 kcal/mol). This seems the main reason that too small a Pt–F bond energy (22.3 kcal/mol) is estimated from eq 12. (b) The Pt–H bond energy can also be estimated by considering reactions given below:

$$Pt(PH_3)_2 + SiH_4 \rightarrow cis\text{-}Pt(H)(SiH_3)(PH_3)_2 \quad (13)$$

$$Pt(PH_3)_2 + CH_4 \rightarrow cis\text{-}Pt(H)(CH_3)(PH_3)_2 \quad (14)$$

E(Pt–H) is calculated to be 50.7 kcal/mol from eq 13 and 53.7 kcal/mol from eq 14 at the MP4(SDQ) level. Although these values are slightly smaller than the E(Pt–H) value in Table II, their differences seem tolerable and do not alter the discussion at all.

(38) Golden, D. M.; Benson, S. W. *Chem. Rev.* **1969**, *69*, 125.
(39) Doncaster, A. M.; Walsh, R. *Int. J. Chem. Kinet.* **1981**, *13*, 503.
(40) Ho, P.; Melius, C. F. *J. Phys. Chem.* **1990**, *94*, 5120.
(41) Schlegel, H. B. *J. Phys. Chem.* **1984**, *88*, 6254.
(42) Faber, M.; Srivastava, R. D. *J. Chem. Soc., Faraday Trans. I* **1978**, *74*, 1089.
(43) Walsh, R. *Acc. Chem. Res.* **1981**, *14*, 246.

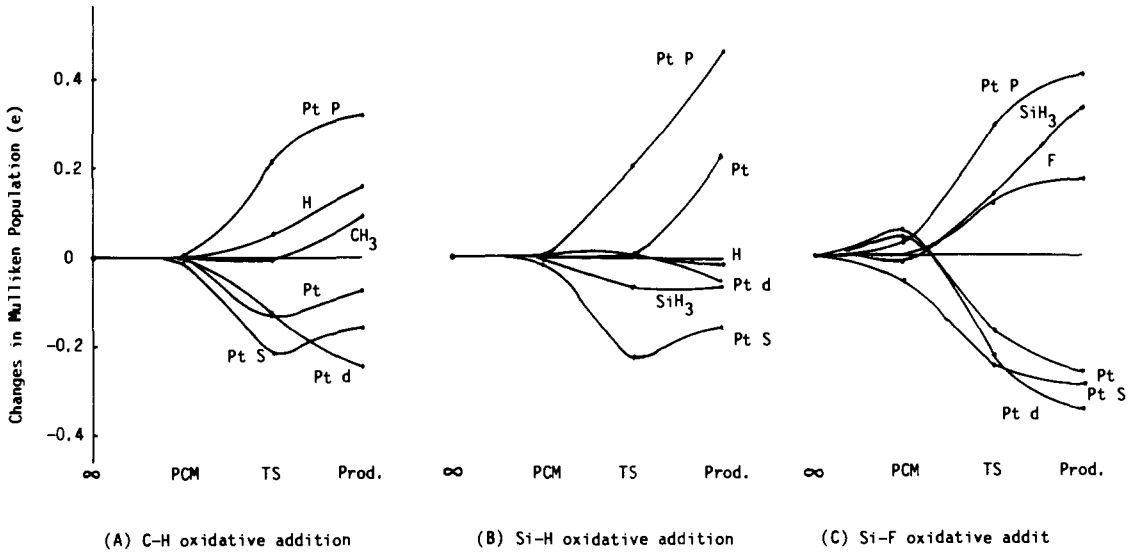

Figure 5. Changes in Mulliken populations caused by C–H, Si–H, and Si–F oxidative additions. Infinite separation is taken as standard (change 0). The positive change means an increase in population, and vice versa.

this bond energy is calculated by considering eq 11. Thus, we must pay attention to the Si–F and Pt–F bond energies in discussing the Si–F oxidative addition.

Now, we have made preparations for comparing the Si–H oxidative addition with the C–H oxidative addition. As shown in Table II, the C–H bond is stronger than the Si–H bond by ca. 15 kcal/mol, while the Pt–CH_3 bond is weaker than the Pt–SiH_3 bond by ca. 20 kcal/mol. Thus, in the C–H oxidative addition, the strong C–H bond is broken and the weak Pt–CH_3 bond is formed, while in the Si–H oxidative addition the weak Si–H bond is broken and the strong Pt–SiH_3 bond is formed. Accordingly, the Si–H oxidative addition easily proceeds, but the C–H oxidative addition occurs with difficulty.

The electron redistribution caused by these oxidative additions exhibits interesting differences between the C–H and Si–H oxidative additions. In the C–H oxidative addition, the electron population of the Pt d orbital significantly decreases, but the electron populations of H and CH_3 considerably increase, as shown in Figure 5 (note a positive value means an increase in Mulliken population and vice versa). In the Si–H oxidative addition, on the other hand, the electron populations of the Pt d orbital and the H atom change only a little, but the electron population of SiH_3 slightly decreases, unexpectedly. These differences are easily interpreted in terms of electronegativities of C and Si. The CH_3 group needs to receive more electrons from Pt because of the large electronegativity of C, while the SiH_3 group does not want to receive further electrons or, rather, donates some of electrons to Pt owing to the small electronegativity of Si. Since the H atom in SiH_4 is almost neutral (0.98e Mulliken population) due to the small electronegativity of Si, the H atom does not need to receive electrons from Pt in the Si–H oxidative addition (0.97e Mulliken population in *cis*-Pt(*H*)(SiH_3)(PH_3)$_2$). However, the H atom in CH_4 is positively charged (0.82e Mulliken population) because of the large electronegativity of C. Thus, the H atom of CH_4 needs to receive electrons from the Pt d orbital in the C–H oxidative reaction (0.97e Mulliken population in *cis*-Pt(*H*)(CH_3)(PH_3)$_2$). Consequently, the electron redistribution is different between the C–H and Si–H oxidative additions, as shown in Figure 5, A and B. From these results, the reaction between CH_4 and $Pt(PH_3)_2$ is clearly characterized as the typical oxidative addition, while the reaction between SiH_4 and $Pt(PH_3)_2$ is considered as the rearrangement of covalent bonds rather than the oxidative addition.

Let us now mention electron populations of the Pt s and p orbitals. The electron population of the Pt p orbital significantly increases and the electron population of the Pt s orbital substantially decreases through both C–H and Si–H oxidative additions, as shown in Figure 5. These changes would arise from the reorganization of the Pt hybridization.[44a] Here, we do not present a detailed explanation because it is irrelevant to the main subject of this work.[44b]

Si–F Oxidative Addition. In the reaction between $R_2FSi–SiFR_2$ and $Pt(PEt_3)_3$, not the Si–F oxidative addition but the Si–Si oxidative addition occurs.[22b] Here, the Si–F oxidative addition is investigated to clarify its reason. In the PCM, the C_{3v} structure **17a** (Figure 6) is more stable than the other three structures (**17b**, **17c**, and **17d** in Scheme I).[45] The stabilization energy of **17a** is about 4 kcal/mol after the BSSE correction (Table I). This value is the greatest in the PCM's examined, which suggests that an electronegative substituent on Si stabilizes the PCM.

The geometry of the TS exhibits several characteristic features, as shown by **7** (Figure 3): (1) the Si–F bond significantly lengthens, and (2) the Pt–F and Pt–Si distances and the PPtP angle are similar in magnitude to those in the product. These features indicate that the Si–F oxidative addition reaches the TS rather late, like the C–H oxidative addition.

Corresponding to these features, the Si–F oxidative addition is endothermic and needs substantially high activation energy (Table I). This result is interpreted again in terms of bond energies. Although the Pt–F bond is stronger than the Pt–H bond, the Si–F bond to be broken is much stronger than the Si–H bond [although the Pt–F and Si–F bond energies are underestimated here (vide supra), the discussion presented is not altered by such underestimation]. Consequently, the Si–F oxidative addition is

(44) (a) The sp hybridization of Pt changes to the dsp^2 hybridization upon going to four-coordinate planar Pt(H)(EH_3)(PH_3)$_2$ (E = C or Si) from Pt(PH_3)$_2$. This means that the Pt p orbitals contribute more to the coordinate bond in the four-coordinate planar complex than in the two-coordinate linear complex, while the Pt s orbital contributes less to the coordinate bond in the four-coordinate planar one than in the two-coordinate linear one. Thus, the Pt p orbital population increases but the Pt s orbital population decreases by the oxidative addition. (b) The Pt s orbital population exhibits an extremum between the PCM and the product in the C–H and Si–H oxidative additions (Figure 5, A and B). One possible reason is the counter intuitive orbital mixing[44c] that often occurs in transition-metal complexes. In fact, the orbital population of the most diffuse s-contracted function increases upon going to the product from the TS. However, we cannot say for certain whether or not it is a solid reason and whether or not there is another true reason, at the present stage. Although the Pt s-orbital population increases upon going to the product from the TS in the C–H and Si–H oxidative additions, the unexpected increase is not so much and the difference in electron redistribution between the C–H and Si–H oxidative additions does not seem to be influenced by this unexpected change. Thus, further discussion is omitted here. (c) Whangbo, M. H.; Hoffmann, R. *J. Chem. Phys.* **1978**, *68*, 5498. Ammeter, J. H.; Burgi, H.-B.; Thibeault, J. C.; Hoffmann, R. *J. Am. Chem. Soc.* **1978**, *100*, 3686.

(45) Only the Pt–Si distance is optimized by least-squares fitting of total energies, where geometries of the $Pt(PH_3)_2$ and SiH_3F parts are fixed to their isolated structures and SiH_3F is placed on the *z*-axis so as to keep the symmetry. The C_s structure like **3b** was not examined because the C_s and C_{3v} structures (**3a** and **3b**) yield almost the same stabilization energy.

Scheme I

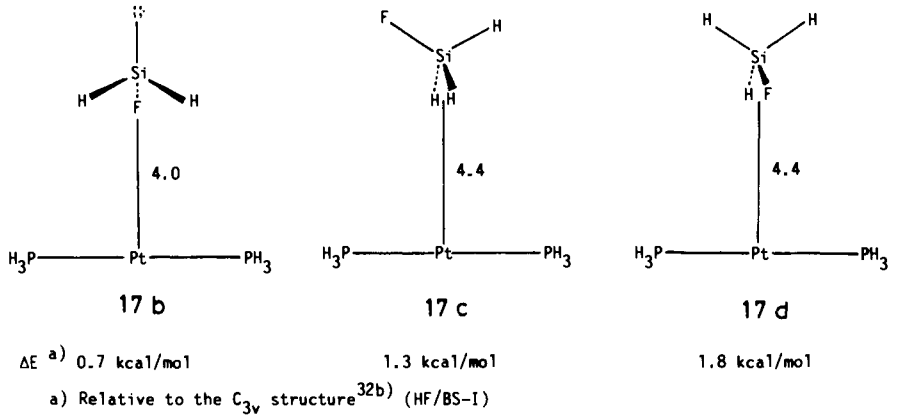

Scheme II

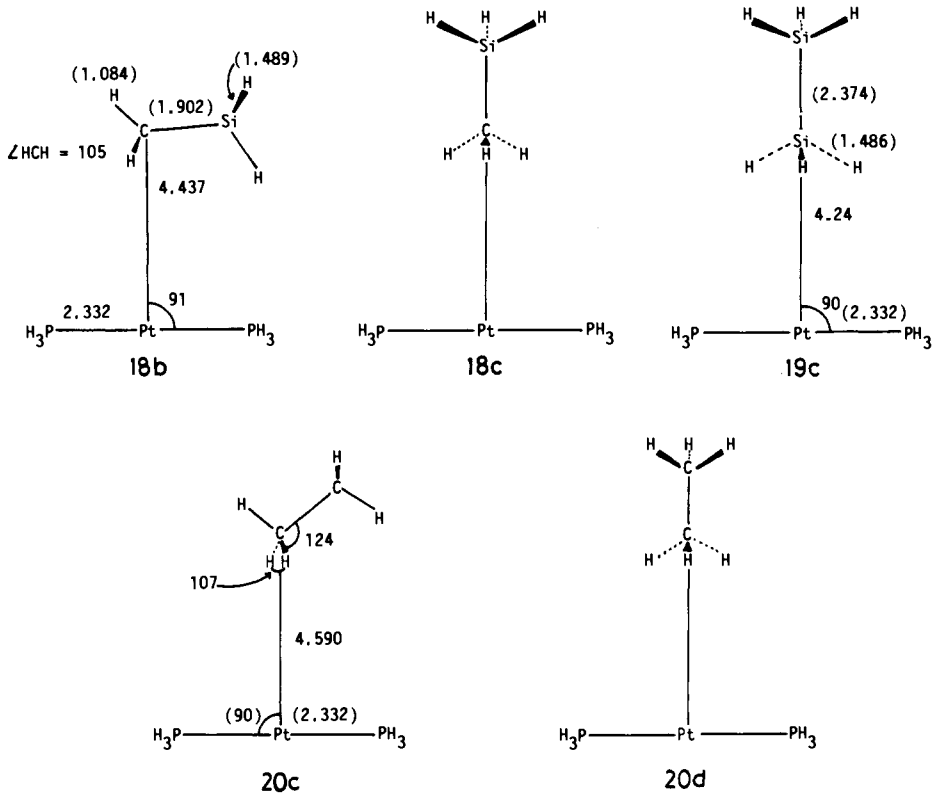

endothermic and needs substantially high activation energy to break the Si–F bond.

The electron redistribution caused by this Si–F oxidative addition essentially differs from that in the Si–H oxidative addition. As shown in Figure 5C, the electron population of the Pt d orbital decreases considerably, but the electron populations of F and SiH_3 remarkably increase by this oxidative addition, as in the C–H oxidative addition. This electron redistribution is easily understood by considering the large electronegativity of the F atom. The F atom in SiH_3F does not possess enough electron population (9.43e) to satisfy its large electronegativity, and, at the same time, the SiH_3 group in SiH_3F is short of electron population (16.57e) because of the large electronegativity of the F atom; accordingly, electron populations of both F and SiH_3 increase, but the Pt d-orbital population decreases by the Si–F oxidative addition. From these features, the reaction of SiH_3F with $Pt(PH_3)_2$ is characterized as the oxidative addition.

CH_3–CH_3, SiH_3–CH_3, and SiH_3–SiH_3 Oxidative Additions. There are many possible structures of PCM's (see Figure 6 and Scheme II for the most stable structure and less stable ones, respectively). In the PCM of $Pt(PH_3)_2(Si_2H_6)$, **19a** and **19b** (Figure 6) yield almost the same stabilization energy, and they are more stable than **19c** (Scheme II).[46] In $Pt(PH_3)_2(SiH_3CH_3)$, **18a** (Figure 6) is 1.7 kcal/mol (MP4/SDQ) more stable than **18b** (Scheme II).[47a] In $Pt(PH_3)_2(C_2H_6)$, **20a** and **20b** (Figure 6) yield almost the same stabilization energy and they are 0.6 kcal/mol more stable than **20c** (Scheme II).[47b] Stabilization energies of all these PCM's are very small as shown in Table I (1.0 ~ 2.6 kcal/mol after the BSSE correction), and their interfragment distances are remarkably long. These features again indicate that these PCM's are characterized as a van der Waals complex.

Several interesting features are found in the geometries of the TS (Figure 3). (1) In the C–C oxidative addition, the C–C bond distance considerably lengthens and the PPtP angle remarkably

(46) Only the Pt–Si distance is optimized by least-squares fitting of total energies, where geometries of the Si_2H_6 and $Pt(PH_3)_2$ parts are taken to be the same as their isolated structures. A thus-optimized structure is less stable than **19a** and **19b** by 0.3 kcal/mol (HF/BS-I).

(47) (a) **18b** is optimized with the energy gradient technique at the HF level. The C_s structure **18c** (Scheme II), in which the CH_3 group approaches Pt, is not examined because the corresponding C_s structure of $Pt(PH_3)_2(CH_4)$ is less stable than the C_2 structure **4**. (b) In $Pt(PH_3)_2(C_2H_6)$, the C_s structure (**20c**) is not examined because the C_s structure of $Pt(PH_3)_2(CH_4)$ is less stable than the C_2 one (see text).

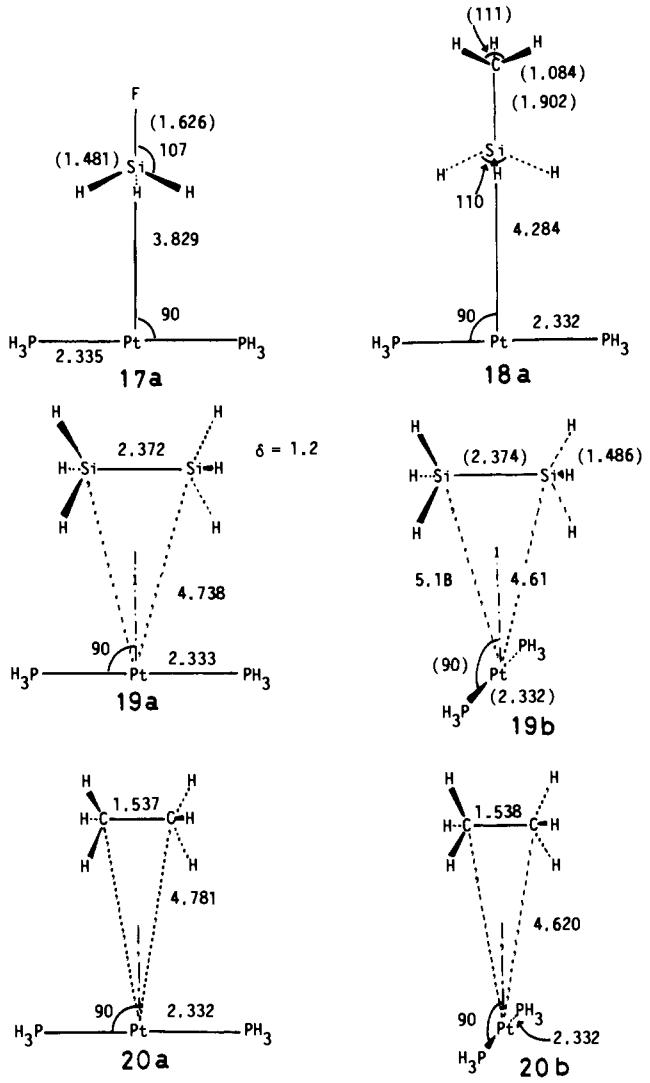

Figure 6. Optimized geometries of precursor complexes, $Pt(PH_3)_2(Si-H_3F)$, $Pt(PH_3)_2(SiH_3-CH_3)$, $Pt(PH_3)_2(SiH_3-SiH_3)$, and $Pt(PH_3)_2-(CH_3-CH_3)$: distances in Å and angles in deg. In parentheses are assumed values which are taken to be the same as in the free molecule.

closes, while the Pt–C distance is still long. (2) In the Si–C and Si–Si oxidative additions, the Si–C and Si–Si distances moderately lengthen, while the Pt–Si and Pt–C distances are still long, compared to the product. (3) The PPtP angle closes in the Si–C and Si–Si oxidative additions, to a lesser extent, than in the C–C oxidative addition. (4) The CH_3 and SiH_3 groups are beginning to turn the direction of their sp^3 orbital toward the Pt atom; accordingly, their directions are almost the medium between directions of Pt–Si (or Pt–C) and Si–Si (Si–C or C–C) bonds. These features suggest that the C–C, Si–C, and Si–Si bonds are going to be broken, but the new Pt–C and Pt–Si bonds are still not formed at the TS. Because the PPtP angle decreases to 97–98° from 180° upon going to the product from the reactant, this angle can be taken here as a measure of the TS character. The PPtP angle is the least closed in the Si–Si oxidative addition but the most closed in the C–C oxidative addition. These results suggest that the Si–Si oxidative addition reaches the TS earliest, but the C–C oxidative addition gets to the TS latest in these three reactions.

As shown in Table I, the C–C oxidative addition is endothermic and needs the highest activation energy. The Si–C and Si–Si oxidative additions are exothermic, but they also require higher activation energies than the Si–H oxidative addition. The activation energy increases in the order Si–Si < Si–C < C–C oxidative additions and the exothermicity decreases in the order Si–Si > Si–C > C–C. These results can be successfully interpreted in terms of bond energies again. The Si–Si bond energy is the least, but the C–C bond energy is the greatest in these Si–Si, Si–C, and C–C bonds (see Table II). The Pt–SiH_3 bond is stronger than the Pt–CH_3 bond, as described above. Thus, the Si–Si oxidative addition is the most exothermic and its activation energy is the lowest in these reactions, while the C–C oxidative addition is endothermic and requires the greatest activation energy.

Several interesting differences in the electron redistribution are found in these oxidative additions (Figure 7); in the C–C and Si–C oxidative additions, the electron population of the Pt d orbital remarkably decreases, but electron populations of CH_3 and SiH_3 considerably increase. In the Si–Si oxidative addition, on the other hand, electron populations of the Pt d orbital and the SiH_3 group change only a little. These differences result from the larger electronegativity of C than that of Si, again; in the C–C oxidative addition, the CH_3 group needs to receive electrons from Pt because of the large electronegativity of C. In the Si–Si oxidative addition, SiH_3 does not need to receive further electrons or, rather, slightly donates electrons to Pt, owing to the small electronegativity of Si. In SiH_3-CH_3, SiH_3 is short of electron population but CH_3 possesses more electrons than in CH_3-CH_3, because electrons of SiH_3 are withdrawn to CH_3. In the Si–C oxidative addition, therefore, the electron population of CH_3 increases, to a lesser extent than in the C–C oxidative addition, and the electron

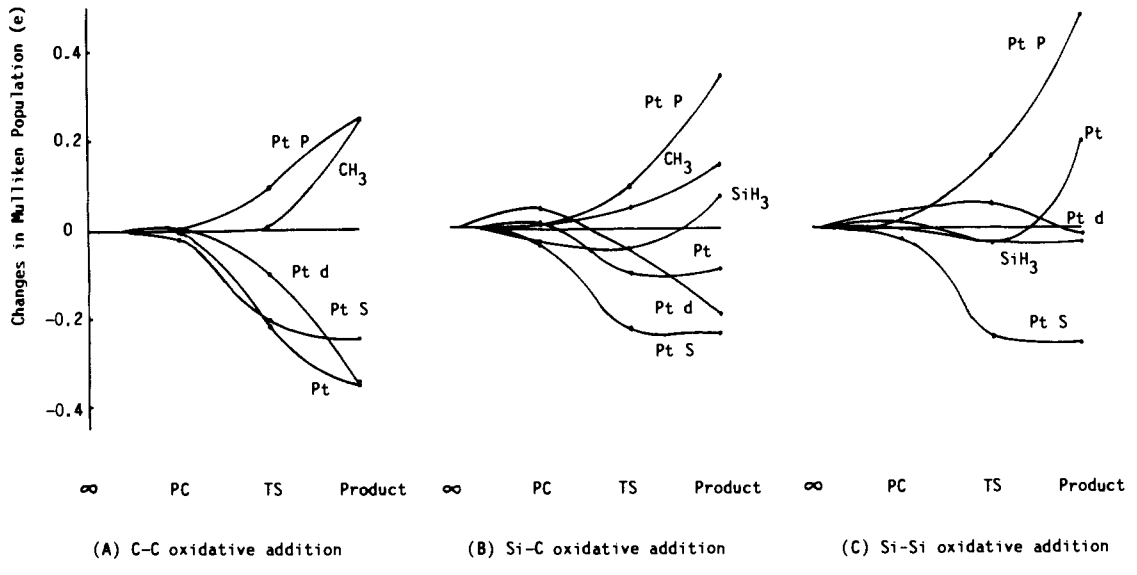

Figure 7. Changes in Mulliken populations caused by C–C, Si–C, and Si–Si oxidative additions (see footnote to Figure 5).

Scheme III

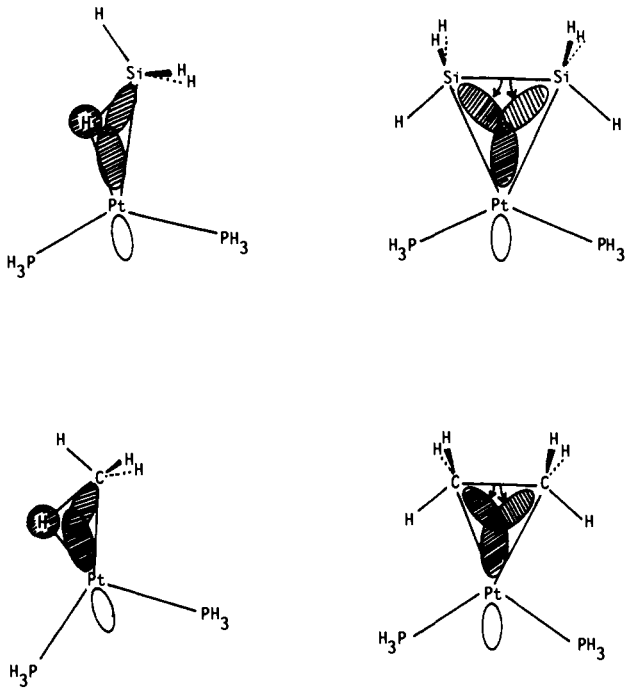

population of SiH_3 slightly increases unlike that in the Si–Si oxidative addition. Again, the C_2H_6 reaction with $Pt(PH_3)_2$ can be clearly characterized as the oxidative addition, while the Si_2H_6 reaction is considered as the rearrangement of covalent bonds rather than the oxidative addition.

Comparison between Si–H and Si–Si Oxidative Additions. Although the Si–Si oxidative addition is much more exothermic than the Si–H oxidative addition, the activation barrier of the former is much higher than that of the latter, as clearly shown in Table I. The higher activation barrier of the Si–Si oxidative addition cannot be interpreted in terms of bond energies, as follows: from bond energies, the Si–Si oxidative addition is predicted to proceed with the lower activation barrier than the Si–H oxidative addition because the Si–Si bond is weaker than the Si–H bond and the Pt–SiH_3 bond is stronger than the Pt–H bond, as shown in Table II (note that one Pt–H and one Pt–SiH_3 bond are formed by the Si–H oxidative addition, but two Pt–SiH_3 bonds are produced by the Si–Si oxidative addition). This prediction contradicts the higher activation energy of the Si–Si oxidative addition. However, one can find an adequate reason by inspecting geometries of the TS. At the TS of the Si–H oxidative addition, the SiH_3 group shifts the direction of its sp^3 orbital by only 9° from the direction of the Si–H bond toward the direction of the Pt–Si bond, as shown in Scheme III. At the TS of the Si–Si oxidative addition, on the other hand, the SiH_3 group turns the direction of its sp^3 orbital by 29° from the direction of the Si–Si bond toward the direction of the Pt–Si bond. This difference results from the fact that the 1s valence orbital of H is nondirectionally spherical, but the sp^3 valence orbital of SiH_3 is directional.[48] In the Si–H oxidative addition, the H atom can form the new Pt–H bond without breaking the Si–H bond because of its spherical 1s valence orbital. At the same time, the H atom can closely approach the Pt atom because of its small size. Consequently, the TS takes the structure **6** (Figure 3), in which the sp^3 orbital of SiH_3 can form the new bond with the Pt atom by changing slightly its direction, as schematically shown in Scheme III. In the Si–Si oxidative addition, on the other hand, the highly directional sp^3 orbital of SiH_3 can form a new bond with the Pt atom, only if its direction is changed toward the Pt atom. Thus, SiH_3–SiH_3 must cause a large distortion at the TS, which considerably destabilizes SiH_3–SiH_3 in energy. As shown in Figure 8, the destabilization energy of SiH_4 is only 1.2 kcal/mol (MP4/SDQ) at the distortion angle of 9°, while the destabilization energy of SiH_3–SiH_3 is 14.4 kcal/mol (MP4/SDQ) at the distortion angle of 29°. The difference in the destabilization energy between them roughly corresponds to the difference in the activation barrier between Si–H and Si–Si oxidative additions.

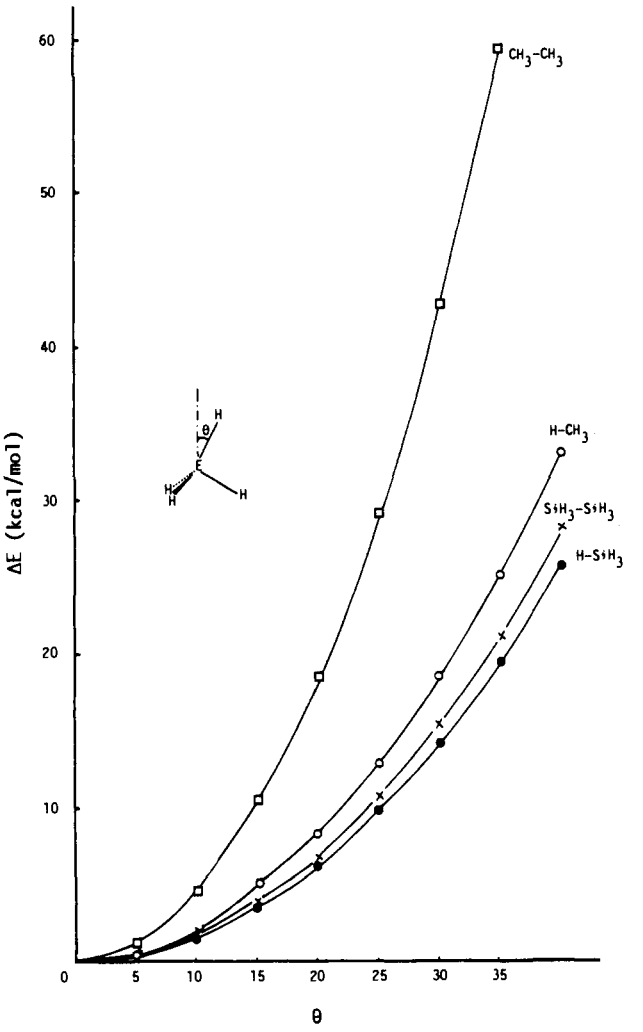

Figure 8. Distortion energies of CH_3–CH_3, H–CH_3, SiH_3–SiH_3, and H–SiH_3: MP4(SDQ)/BS-II calculation.

Quite the same situation is found in the comparison between the C–H and C–C oxidative additions. As shown in Table I, the C–C oxidative addition needs significantly higher activation energy than the C–H oxidative addition, while both are similarly endothermic. In the C–C oxidative addition, the CH_3 group must change the direction of its sp^3 orbital to form the new bond with the Pt atom, which causes a considerably large distortion of CH_3–CH_3 and remarkably weakens the C–C bond as does the SiH_3 group in the Si–Si oxidative addition. In the C–H oxidative addition, on the other hand, the H and CH_3 groups can form new bonds with the Pt atom by causing a smaller distortion than in the C–C oxidative addition. The distortion angle of CH_3–CH_3 at the TS is 33°, but that of CH_4 is 26°. Distortion energies of CH_3–CH_3 and CH_4 are about 53 and 14 kcal/mol (MP4/SDQ), respectively. Again, the difference between them roughly corresponds to the difference in the activation energy between C–H and C–C oxidative additions.

In conclusion, the activation energies of Si–Si and C–C oxidative additions depend not only on bond energies but also on distortion energies.

Comparison of Si–F, Si–H, and Si–Si Oxidative Additions. The Si–F oxidative addition is moderately endothermic, but the Si–Si oxidative addition is significantly exothermic. Additionally, the

(48) Essentially the same discussion has been presented in the previous theoretical reports of H–H, H–CH_3, and CH_3–CH_3 oxidative additions to transition metals.[3b,8d,e,9b,c]

former needs a higher activation energy than the latter. From these results, the Si–Si oxidative addition is predicted to proceed more easily than the Si–F oxidative addition. This prediction agrees well with the experimental result that not the Si–F but the Si–Si oxidative addition occurs in the reaction between R_2SiF–$SiFR_2$ and $Pt(PEt_3)_3$.[22b]

The comparison between Si–H and Si–Si oxidative additions is also interesting; as described above, the Si–Si oxidative addition is significantly exothermic but needs an activation energy of 19.6 kcal/mol. The Si–H oxidative addition, on the other hand, proceeds with a very small activation barrier, but it is less exothermic than the Si–Si oxidative addition. These results indicate which occurs, the Si–H or the Si–Si oxidative addition, depends on the reaction conditions when the substrate involves both Si–H and Si–Si bonds such as R_2SiH–$SiHR_2$. If the reaction conditions are very mild, only the Si–H oxidative addition would proceed. However, if the reaction conditions are not very mild, the Si–Si oxidative addition proceeds to yield $Pt(SiHR_2)_2(PR'_3)_2$ as a product, probably after the mutual conversion between $Pt(H)(SiR_2–SiHR_2)(PR'_3)_2$ and $Pt(PR'_3)_2 + R_2SiH–SiHR_2$. This discussion can account for several experimental results that the reaction of $R_2HSi–SiHR_2$ with $Pt(PR'_3)_2$ produces $Pt(SiHR_2)_2(PR'_3)_2$ as a product[24,49] after formation of the short-lived $Pt(H)(SiR_2–SiHR_2)(PR'_3)_2$.[50]

Concluding Remarks

Compared to the C–H oxidative addition, the Si–H oxidative addition proceeds very easily because the Si–H bond is weaker than the C–H bond, but the Pt–SiH_3 bond is stronger than the Pt–CH_3 bond. The other striking differences to be noted are found in the electron redistribution. In the C–H oxidative addition, the Pt d-orbital population significantly decreases, but electron populations of H and CH_3 groups remarkably increase. These changes in electron distribution are consistent with our understanding that this reaction is characterized as the typical *oxidative addition*. In the Si–H oxidative addition, however, electron populations of the Pt d orbital, H, and SiH_3 change only a little, which comes from the fact that the Si atom is less electronegative than the C atom. Thus, the Si–H oxidative addition is considered as the *rearrangement of covalent bonds* rather than the oxidative addition.

Although the Si–H oxidative addition proceeds easily, the Si–F oxidative addition is very difficult because the strong Si–F bond should be broken. The reaction between F–SiH_3 and $Pt(PH_3)_2$ is characterized as an *oxidative addition* because of the large electronegativity of F. In the C–C, Si–C, and Si–Si oxidative additions, the activation barrier increases in the order Si–Si < Si–C < C–C, and the exothermicity decreases in the order Si–Si > Si–C > C–C. This order of the reactivity is also successfully understood by considering the bond energies of Si–Si, Si–C, C–C, Pt–CH_3, and Pt–SiH_3. Differences in the electron redistribution of these reactions are successfully interpreted in terms of electronegativities of C and Si. Again, the CH_3–CH_3 reaction with $Pt(PH_3)_2$ is characterized as an *oxidative addition*, while the SiH_3–SiH_3 reaction is considered as a *rearrangement of covalent bonds*.

Compared to the Si–H oxidative addition, the Si–Si oxidative addition needs significantly high activation energy in spite of its large exothermicity, which mainly results from the distortion of SiH_3–SiH_3 at the TS; because the sp^3 valence orbital of SiH_3 is highly directional, the SiH_3 group must shift the direction of its sp^3 orbital toward the Pt atom, to form a new bond with the Pt atom, which is the major cause of the significant distortion of SiH_3–SiH_3. As a result, the Si–Si oxidative addition needs a high activation energy. In the Si–H oxidative addition, on the other hand, the Pt–H bond can be formed without breaking completely the Si–H bond because the H atom has a spherical 1s valence orbital. At the same time, the H atom can closely approach the Pt atom owing to its small size. Consequently, the TS of this reaction takes the structure **6** (Figure 3), in which the SiH_3 group does not need to shift the direction of its sp^3 orbital so much. Thus, the Si–H oxidative addition can proceed with the small activation barrier.

In summary, one can predict from bond energies whether the Si–X oxidative addition proceeds easily or not, when X has a spherical valence orbital like H and halogen. When X′ has a directional valence orbital like CH_3 and SiH_3, the exothermicity of the Si–X′ oxidative addition can be easily predicted from bond energies, but the activation energy is higher than that predicted from bond energies because the Si–X′ bond must be distorted at the TS to make new bonds with the Pt atom. Thus, the activation energy of the oxidative addition cannot be compared, in general, between Si–X and Si–X′ bonds.

Acknowledgment. This work was supported by grant from the Ministry of Education, Culture, and Science, Japan (No.04243102). Calculations were carried out by using the Hitach S-820 Computer of the Institute for Molecular Science.

(49) (a) In the reaction of $R_2SiH–SiHR_2$ with $Pt(PR'_3)_2$, $Pt(SiHR_2)_2(PR'_3)_2$ is experimentally obtained as a product.[49b] (b) Yamashita, H.; Tanaka, M.; Goto, M. *Organometallics*, in press.

(50) (a) In the reaction of $R_2SiH–SiHR_2$ with Pt(0), the product of the Si–H oxidative addition is formed first, but the product of the Si–Si oxidative addition is finally obtained.[50b] (b) Fink, M.; Recatto, C. A.; Michalczyk, M. J.; Calabrese, J. C. The 25th Silicon Symposium, Los Angeles, April 1992.